Journal of Physics: Conference Series **550** (2014) 012038 doi:10.1088/1742-6596/550/1/012038

Experimental investigation of filamentary and non-filamentary regimes in a surface dielectric barrier plasma actuator

I Biganzoli[1], R Barni[1], A Gurioli[2], R Pertile[2] and C Riccardi[1]

[1] Dipartimento di Fisica G. Occhialini, Università degli Studi di Milano-Bicocca, piazza della Scienza 3, 20126, Milano, Italy

[2] Aerodynamics & Wind Tunnel Departments, Alenia Aermacchi SPA, via Ing. Foresio 1, 21040, Venegono Superiore (VA), Italy

E-mail: claudia.riccardi@mib.infn.it

Abstract. Asymmetric surface dielectric barrier discharges fed by a high-voltage sinusoidal low-frequency drive are currently proposed as plasma actuators, because they can induce a directed airflow in the gas surrounding the surface. However, it is known that the induced airflow speed can not be increased as much as desired because a saturation is generally observed for sufficient high voltages. In this paper we show that when the voltage amplitude is increased enough the discharge does not appear uniform any more, but a pattern of plasma filaments becomes evident. We have thus studied plasma properties in both filamentary and non-filamentary regimes, by means of a Rogowski coil for the measurement of the current associated to the discharge. This is interesting in order to understand what happens at high voltages, when the saturation of the induced airflow speed occurs.

1. Introduction

When a sufficiently high voltage difference is applied between two electrodes placed at the opposite sides of an insulating material, a Surface Dielectric Barrier Discharge (SDBD) is obtained because of the ionization of the gas surrounding the dielectric material [1]. If one electrode is insulated, plasma is created in correspondence of just one side of the barrier (Figure 1). With this geometrical configuration and in air at atmospheric pressure, SDBDs are used as plasma actuators, for the manipulation of the boundary layer of an airflow surrounding a body, and thus in the active flow control field [2]. As a matter of fact, these non-thermal plasmas can generate an induced airflow of some m/s that can interact with an external wind, thus providing, for instance, stall prevention, lift enhancement or drag reduction [3, 4]. Presently, these applications in the aeronautical sector are interesting but partially limited by the fact that the induced airflow speed cannot be increased as much as desired because a saturation in the induced wind velocity is generally observed at sufficiently high voltages [5].

It is known that, when the electric field created by the voltage difference imposed between the electrodes is sufficiently high, plasma is created and electrical charges are transported through the gap and accumulated on the insulating surfaces [6]. This charge accumulation generates an electric field that locally weakens the external one. When the total electric field falls below the threshold necessary for plasma ignition, the discharge extinguishes. If the voltage imposed to

Content from this work may be used under the terms of the Creative Commons Attribution 3.0 licence. Any further distribution of this work must maintain attribution to the author(s) and the title of the work, journal citation and DOI.
Published under licence by IOP Publishing Ltd

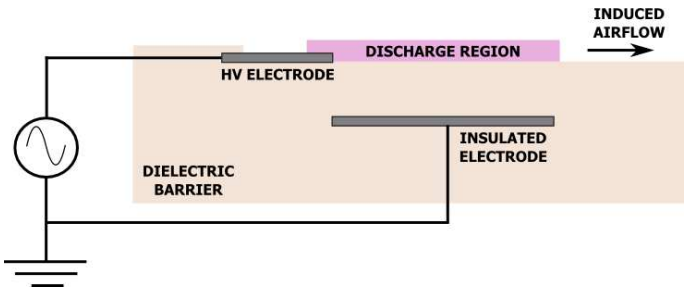

Figure 1. Schematic of a Surface Dielectric Barrier Discharge configuration.

the fed electrode is increased, the discharge can be locally initiated again, and that is the reason why a sinusoidal high-voltage supply is adopted instead of a continuous one. Consequently, the presence of the insulating barrier usually leads to a regime where charge is mainly transported in sub-millimetre regions consisting of current filaments with temporal duration limited to a few tens of nanoseconds [7]. These plasma *microdischarges* are concentrated into two phase intervals of the sinusoidal voltage supply, when the modulus of the applied voltage difference is high enough and is increasing in time. These two phases of plasma activity are often called *Backward Stroke* (BD) and *Forward Stroke* (FD), depending if the voltage difference between the fed electrode and the grounded one is rising from its minimum to its maximum or decreasing from its maximum to its minimum [8].

In a previous work we have point out that not all plasma properties of the two semi-cycles must be identical, because of the asymmetrical configuration adopted, and that plasma microdischarges emit light for few nanoseconds and carry current for some tens of nanoseconds [5]. We can think that light and current signals give insights about different microdischarge properties. Light is presumably ascribable to electrons that excite nitrogen immediately after the passage of the ionizing wave that initiates the microdischarge. In contrast, the current signal is probably due to the movement of charges into the plasma channel and thus reflects the microdischarge temporal evolution, rather than its formation. Since we are interested in better understanding which plasma characteristics are responsible for the induced airflow generation and saturation, in this paper we have decided to focus on the electrical properties of plasma microdicharges generated during the two strokes, and a Rogowski coil has thus been adopted for current measurements.

We have noticed that when the voltage amplitude is increased enough the discharge does not appear uniform, but a pattern of plasma filaments becomes evident (Figure 2). We have thus studied plasma properties in both filamentary and non-filamentary regimes.

2. Experimental Setup and Diagnostics

In the surface configuration studied in this work, the electrodes are tin clad copper adhesive tapes (60 μm thick and 200 mm long) placed at the opposite sides of a flat dielectric panel (teflon, 2 mm thick), without overlapping. The insulated electrode is 10 mm wide, whereas the air exposed one is just 5 mm wide. An insulating polyisobutylene self-amalgamating tape is used for avoiding discharges at the lower electrode side, but also upstream of the exposed electrode and at the electrode ends. Different voltages (up to about 15 kV peak amplitude) has been tested, at the same frequency (16 kHz). The buried electrode is grounded and the exposed one is fed by a high-voltage power supply, which was the MiniPuls 6 by GBS Elektronik GmbH, consisting of a transistor bridge followed by a transformer cascade [9].

Plasma current microdischarges have been experimentally studied with a sufficiently high temporal resolution by means of home-made Rogowski coils, as described in detail in Section

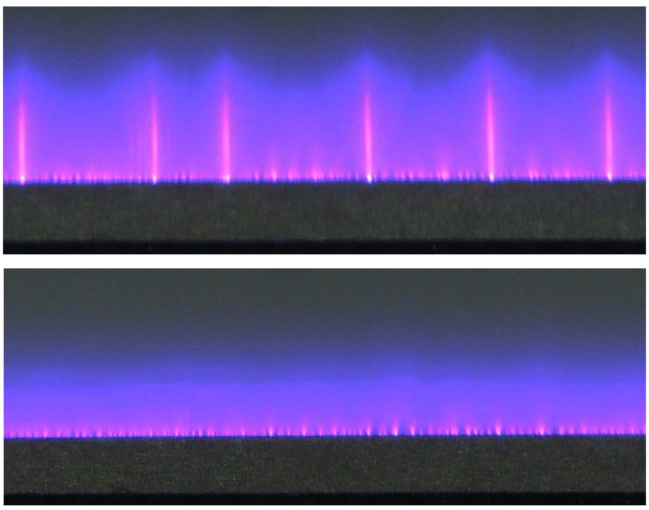

Figure 2. Examples of a SDBD working in non-filamentary (bottom) and filamentary (top) regimes. These pictures were taken from above the discharge, with a commercial digital camera.

2.1. A commercial HV probe (Tektronix P6015A, granted for a bandwidth of 75 MHz) was instead employed for evaluating the voltage at the exposed electrode. The outputs of all these probes were connected to different channels of a large bandwidth digital oscilloscope (Agilent MSO8104A with sampling rate equal to $2\,GSas^{-1}$) and their signals were acquired simultaneously. The presence or absence of discharge disuniformities (plasma filaments) was verified with a commercial digital camera and with a thermal infrared camera FLIR ThermaCAM SC640 (spectral range $7.5 \div 13$ μm). The camera records the infrared emission of the dielectric surface, which is a function of its temperature, and it was placed about 50 cm above the discharge.

Finally, the average fluid dynamic effects induced by the plasma actuator were investigated using a Pitot tube connected to an LPM-9381 Druck transducer that records the differential pressure from which the flow velocity was derived. The single Pitot tube could be replaced by a series of three or more connected capillaries, in order to take a measurement of the flow velocity averaged along the electrode length. In our experiments the Pitot tubes were small glass tubes with outer and inner diameters equal to 1.4 mm and 1.0 mm respectively. The Pitot inlets were placed in contact with the electrode surface, 10 mm downstream the exposed electrode edge, in correspondence of the end of the buried electrode.

2.1. Rogowski Coils

A current transducer like a Rogowski coil is suitable to measure electric current filaments [10]. In a DBD, the electric current flowing into the circuit can be viewed as the superimposition of a low-frequency sinusoidal capacitive current, which is almost independent of plasma presence in the gap, and a discharge current, which is associated with plasma microdischarges and appears as a series of fast current pulses. A Rogowski coil is a conducting wire that is wound in a spiral around a magnetic core and then returns to the original point [11]. The coil is placed around the cable connecting the buried electrode to the ground: any variation in the current I flowing into the cable generates an electromotive force at the output of the coil. By adding an integrating circuit, the output of the probe is proportional to I. We have built a few home-made Rogowski coils and calibrated them in the frequency range $10 \div 100$ MHz, as discussed in a dedicated paper [10]. Since we are mainly interested in the current signal associated with plasma microdischarges, we can separate this current component from the displacement one by means of a band-pass filter based on the fast Fourier transforms, so that current events due to

plasma microdischarges finally appear as pulses emerging from a noisy base line. At this point they are identified by setting a threshold sufficiently higher than noise spikes. Finally, a baseline is used to evaluate the intensity of peaks, as well as their beginning and end. We were able to study current pulses characteristics like number, amplitude, duration and charge transported [5].

3. Experimental Results

As already stated in the introduction, we noticed that for sufficiently high voltages the discharge does not appear uniform but several plasma filaments become evident. First of all we have used the thermal camera to visualize the voltages at which these filaments are visible. An image was captured about one second after the discharge ignition, for voltage amplitudes in the range $6.5 \div 17$ kV, at steps of 1.5 kV. We found that at 6.5 kV (Figure 3 (a)) and 8 kV the discharge appears quite uniform along electrode length (the so-called spanwise direction). At 9.5 kV the plasma regime changes because some small filaments become evident (Figure 3 (b)). At 11 kV they cover the whole electrode length and are more or less uniformly spaced (Figure 3 (c)). Above 12.5 kV the plasma state changes again because there are longer filaments, which are separated one from the other by a larger spanwise distance (Figure 3 (d)). Eventually, at the

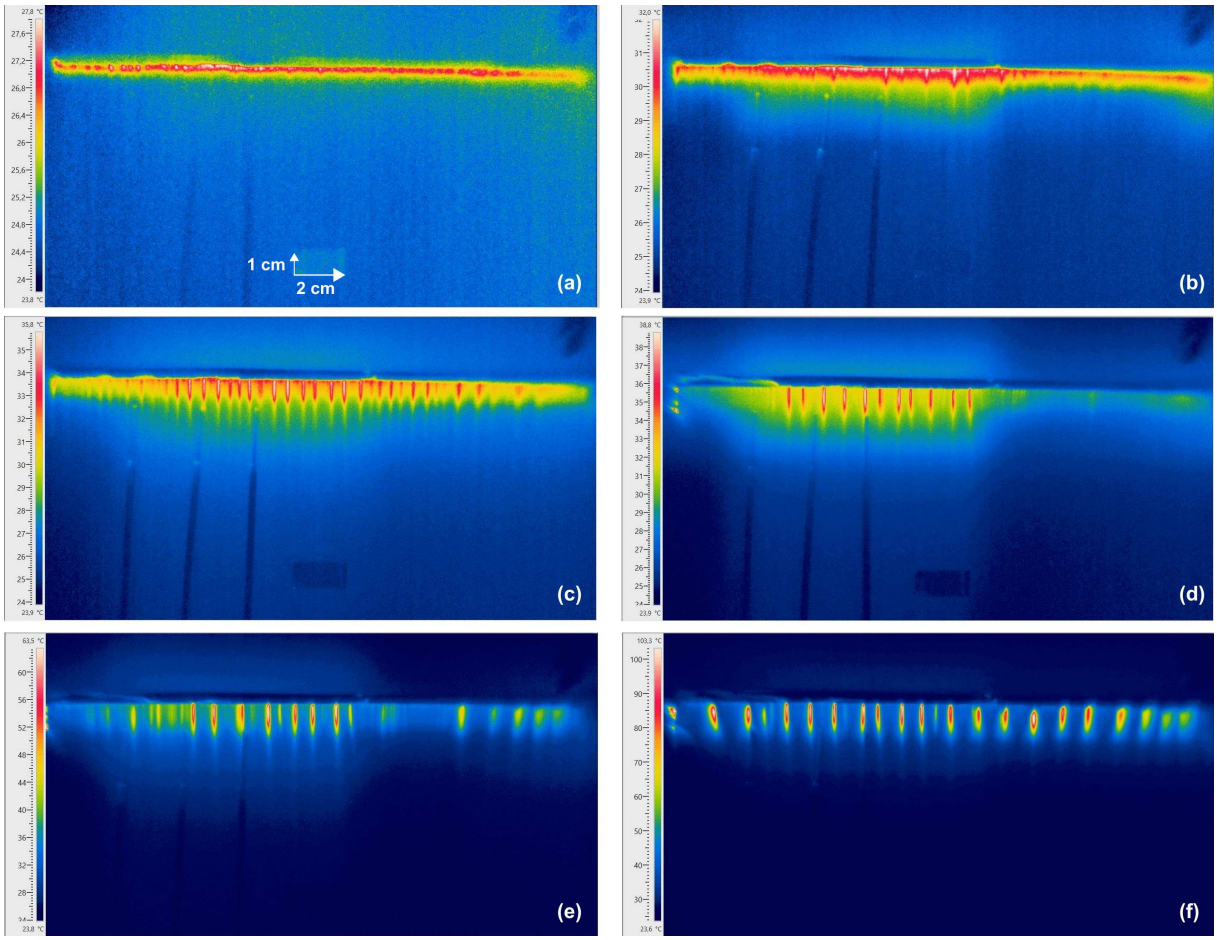

Figure 3. Thermal camera images taken approximately one second after plasma ignition, for different voltage amplitudes: 6.5 kV (a), 9.5 kV (b), 11 kV (c), 12.5 kV (d), 14 kV (e), and 17 kV (f).

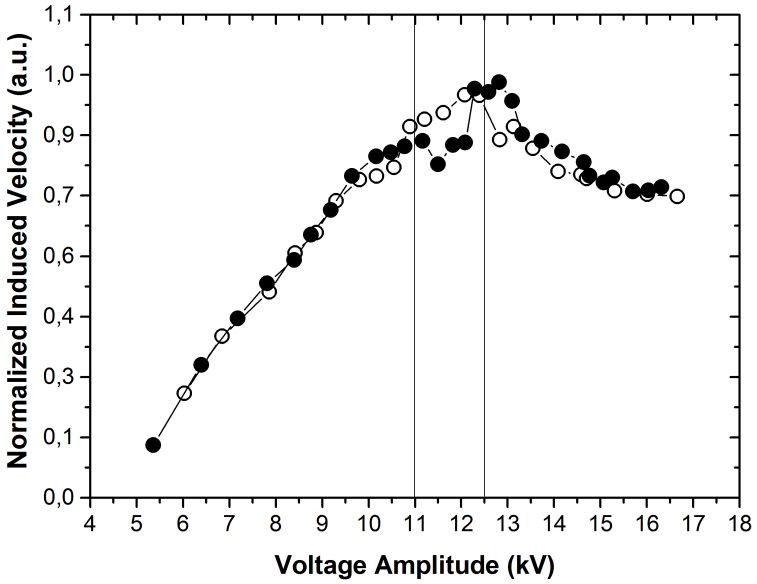

Figure 4. Speed of the induced flow as a function of the applied voltage. Values are normalized to the maximum speed obtained. Full and empty circles are two set of measures, showing a good repeatability and stability of the induced airflow, except in the transition from small to well developed plasma filaments (11÷12.5 kV).

highest voltages (Figures 3 (e) and (f)) these plasma filaments become more numerous. It is evident in subfigures (c), (d) and (e) that the plasma filaments are not uniformly distributed along the spanwise direction, but are more concentrated on the left half of the picture. This is not due to the presence of the Pitot tubes. As a matter of fact, plasma filaments generally change position (moving a few millimetres along the electrode) every some minutes, and we noticed that, if we try to keep a Pitot tube too close to a filament and perfectly in front of it for minutes, this filament motion can be enhanced by the probe presence, because filaments tend to go away from the Pitot tube. In this case, this discharge non-uniformity is instead ascribable to differences in the local dielectric panel temperature before plasma ignition, which was about three degrees higher than the room temperature in the left portion of the panel. For voltages larger than the ones associated to the discharge regime transition, this temperature difference did not influence the spanwise position of filaments, which immediately appeared uniformly distributed as in Figure 3 (f). However, for lower voltage amplitudes, we noticed that the creation of plasma filaments along the whole the electrode length could take some seconds and began from hotter region [12]. These thermal images have been recorded within the first second of plasma actuator operation, and this is the origin of this discharge disuniformity.

During the acquisition of these thermal images we also measured the average speed of the induced airflow by means of three Pitot tubes, which are visible in Figure 3. We then repeated a few more times the measurements of the airflow speed in order to check their repeatability and stability. Two of these measurements are shown in Figure 4. The two curves overlap well, except in the range $11 \div 12.5$ kV, which corresponds to the transition from small filaments to well developed plasma filaments. These curves of the induced wind speed show that any transition in the discharge regime influences the induced flow speed, and thus the potentialities of plasma actuator. It is evident that the the speed of the induced flow increases quite linearly until small filaments appear (in the range $9.5 \div 11$ kV). By using a single glass Pitot tube positioned in front of a plasma filament or in correspondence of the uniform plasma between two filaments, we noticed that at these voltage amplitudes, the induced airflow has a slightly higher speed near a plasma filament rather than where plasma is more uniform. That's why in this region the two curves of Figure 4 do not overlap. However, at higher voltages, the induced flow speed not only saturates but even decreases with the voltage amplitude, and we have observed this trend in front of both uniform plasma regions and plasma filaments. The conclusion that we can

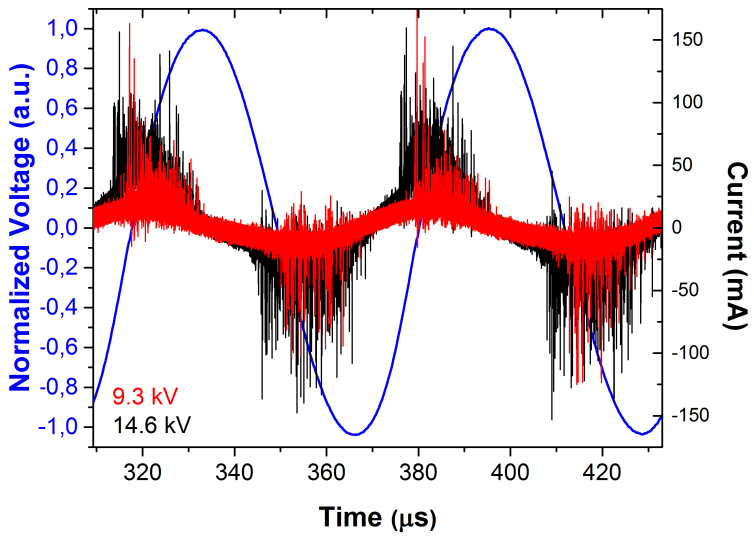

Figure 5. Two current signals obtained at different voltage amplitudes (9.3 kV and 14.6 kV) are shown. A normalized voltage signal is displayed too, as a reference for distinguishing the backward and forward discharges (when the instantaneous voltage rises and decreases respectively).

draw from these experiments is that when the voltage amplitude is increased enough the plasma regime changes from a uniform one to a filamentary one, and there is a transitional range of voltages in which filaments are smaller than the well developed plasma filaments. However, we can think that the formation of filaments is not the only change involved in the plasma regime transition, because at voltages higher than 13 kV, a saturation in the induced wind speed is observed in correspondence of both uniform and filamentary plasma.

Our aim at this point was thus to look for evidences indicating some changes in the plasma state or the appearance of plasma filaments by the analysis of the current microdischarges. In Figure 5 a couple of examples of current signals (before and after the transition) are given together with a reference voltage signal. It is evident that the number of current pulses increases

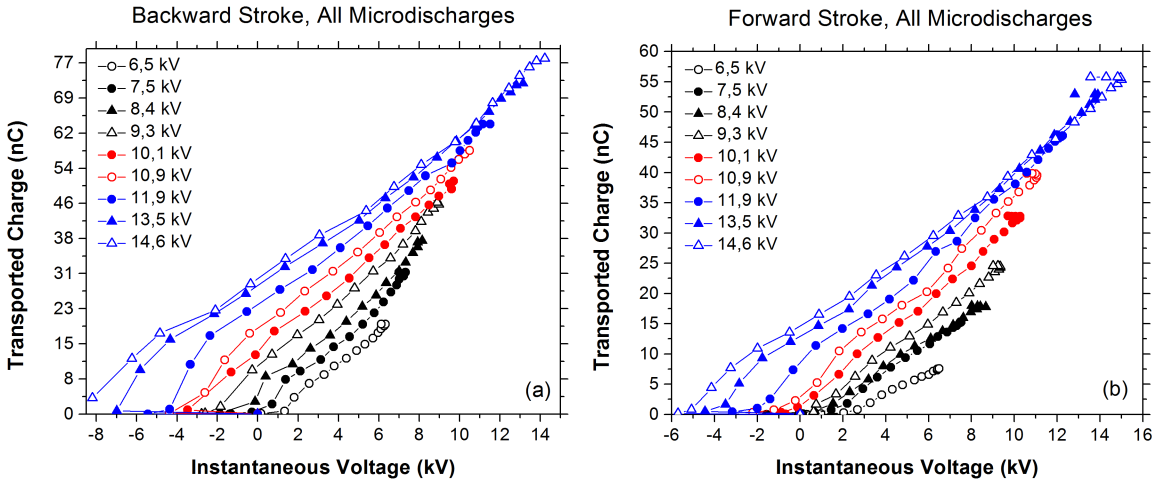

Figure 6. Total charge Q_{micro} that has been moved by current microdischarges already registered during the considered stroke as a function of the voltage V between the electrodes. Figures (a) and (b) refer to the backward and forward discharge respectively, and the different curves are obtained for different voltage amplitudes. Colours indicate the three plasma regimes: uniform plasma (black), uniform plasma with small plasma filaments (red), uniform plasma with well developed plasma filaments (blue).

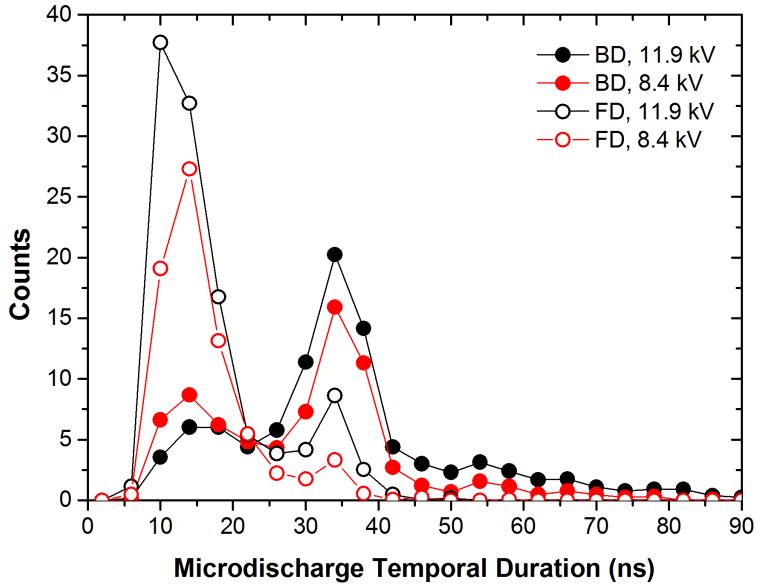

Figure 7. Histograms of the temporal duration of current pulses for the BD and FD strokes. Two different voltage amplitudes are shown (8.4 kV and 11.9 kV).

with the voltage amplitude as well as the sinusoidal current component. We found that the shape of the histogram describing the amplitudes of current microdischarges is almost independent on the applied voltage for the backward discharge, whereas for the forward stroke the histogram tail associated to events with higher amplitudes becomes more accentuated as the voltage amplitude increases. These events could be ascribable to plasma filaments, but further investigations are needed, so this point will be discussed elsewhere. Here we focus on changes in the global behaviour of the forward and backward strokes. For this purpose, for each voltage semi-cycle, we have considered the total charge Q_{micro} that has been moved by current microdischarges already registered during the considered stroke. The trend of Q_{micro} with the instantaneous voltage V applied to the exposed electrode has been considered. In Figure 6 this is plotted for different voltage amplitudes, for both the backward and forward stroke. However, instead of representing the trend of Q_{micro} versus V for a single voltage semi-cycles, we have averaged Q_{micro} over the 13 voltage cycles recorded in a temporal series. At this purpose, instead of considering the instantaneous voltage V at which a single microdischarge happens, we have divided the x-axis in intervals of instantaneous voltages, and we have added up the contributions of all microdischarges recorded at instantaneous voltages falling within the interval. The total values of Q_{micro} obtained in this way for the different voltage intervals have then be divided by 13 so that these plots refer to the average charge transported during a single voltage cycle. Each one of these curves is a $Q-V$ plot similar to the ones considered for Lissajous figures [13], but in this case only the plasma activity phases and only the charge transported by current microdischarges are taken into account. Figure 6 shows that for the three plasma regimes (uniform plasma in black, small filaments in red and plasma filaments in blue), Q_{micro} increases quite linearly with the instantaneous voltage. The voltage amplitude does not seem to influence the slope of this linear increase, but mainly changes the voltage at which breakdown occurs. However, we can notice that immediately after the discharge initiation Q_{micro} increases faster with V. This is the effect of the presence of breakdown microdischarges we have talked about in reference [7]. Eventually, a sort of saturation is noticeable for the highest two voltage amplitudes considered (13.5 and 14.6 kV).

The $Q_{micro} - V$ curves are more interesting if plotted independently for three groups of current microdischarges that can be identified from the histograms of the temporal duration of current microdischarges, which are shown in Figure 7 for both the BD and FD at two different

voltage amplitudes. Three groups of current microdischarges can be identified, whose relative importance depend on the half-cycle considered as well as on the operating voltage amplitude. The first group is made of microdischarges with the shortest temporal duration (less than 25 ns) and we will refer to it as *Group S*. The second group (*Group M*) is made of microdischarges with temporal duration between 25 ns and 45 ns, whereas microdischarges longer than 45 ns belong to the third group (*Group L*). The latter is practically absent for the forward stroke. For the whole range of voltage amplitudes investigated, the number of current pulses belonging to Group S detected during a forward half-cycle is larger than the number of FD microdischarges belonging to Group M. The opposite happens for the backward stroke.

Figures 8 and 9 show the plots of Q_{micro} versus V for these groups of microdischarges

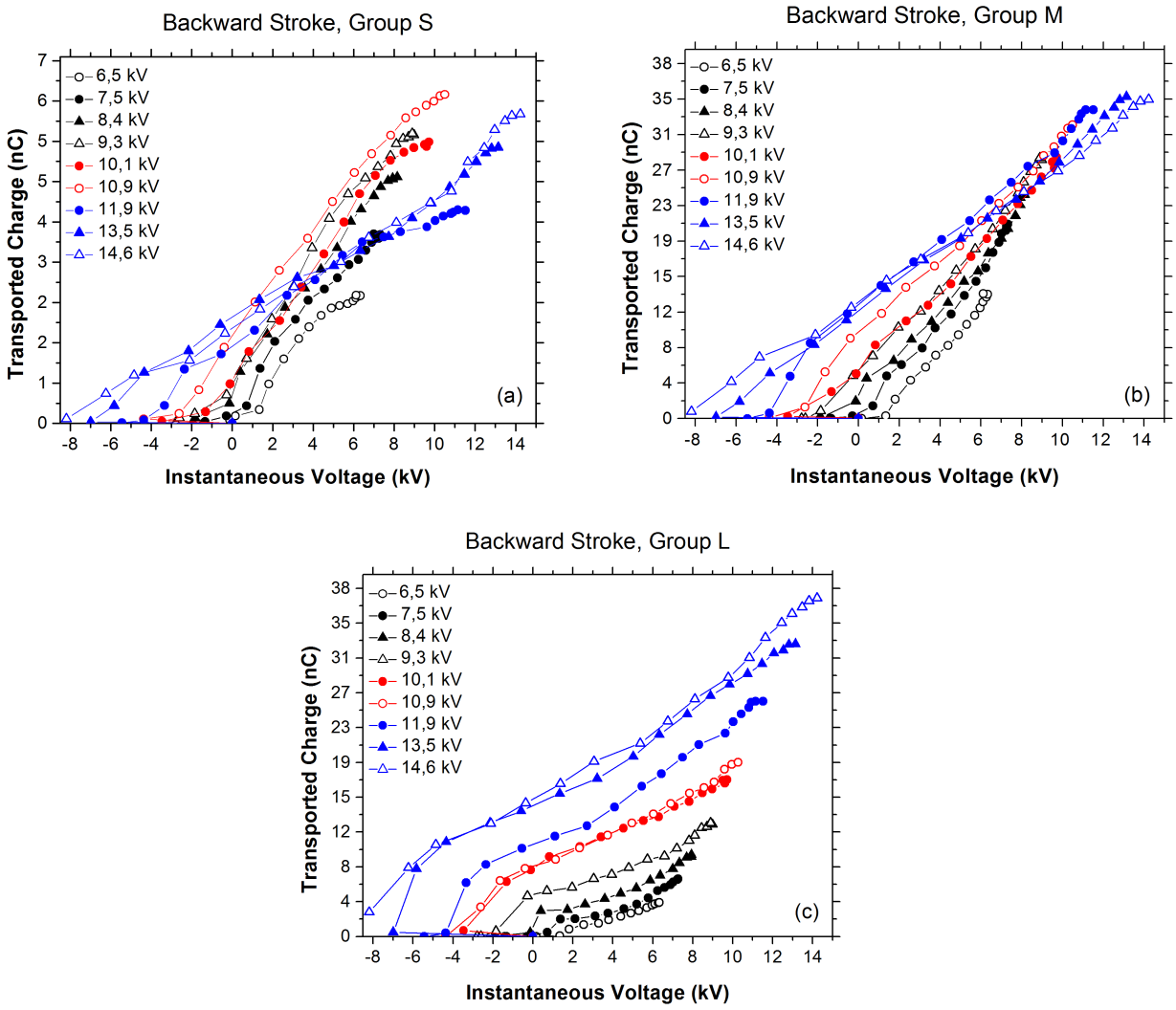

Figure 8. Total charge Q_{micro} that has been moved by BD current microdischarges already registered during the stroke as a function of the voltage V between the electrodes. Figures (a), (b) and (c) refer to microdischarges belonging to Group S, to Group M and to Group L, and the different curves are obtained for different voltage amplitudes. Colours indicate the three plasma regimes: uniform plasma (black), uniform plasma with small plasma filaments (red), uniform plasma with well developed plasma filaments (blue).

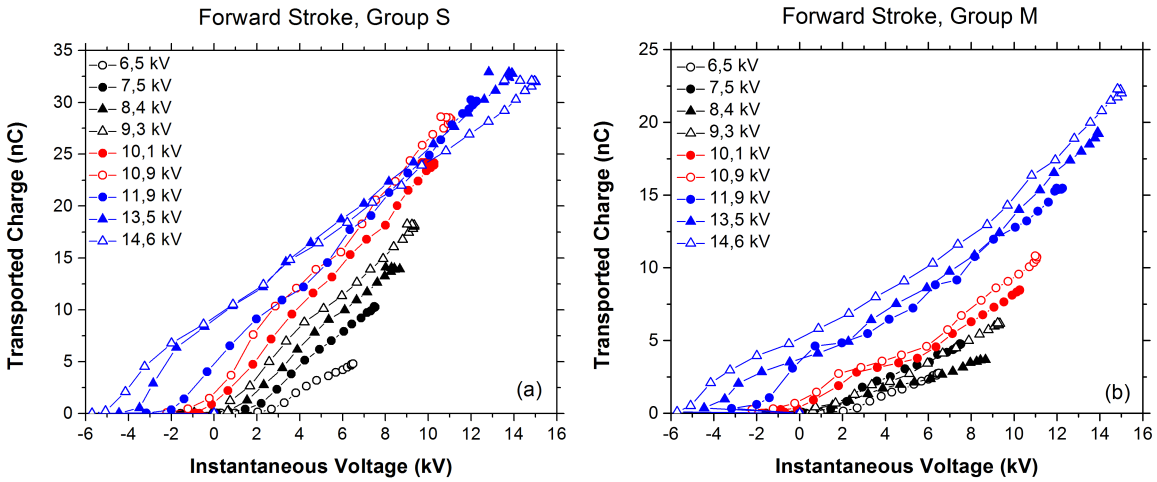

Figure 9. Total charge Q_{micro} that has been moved by FD current microdischarges already registered during the stroke as a function of the voltage V between the electrodes. Figures (a) and (b) refer to microdischarges belonging to Group S and to Group M, and the different curves are obtained for different voltage amplitudes. Colours indicate the three plasma regimes: uniform plasma (black), uniform plasma with small plasma filaments (red), uniform plasma with well developed plasma filaments (blue).

considered independently. We have seen that the trend of Q_{micro} associated to all current microdischarges is not particularly influenced by the voltage amplitude and by the transition to different plasma regimes. On the contrary, we now can see from these figures that, as the voltage amplitude increases, these three groups of plasma microdischarges are favoured or not in different ways. It is evident that for the backward stroke Group S and Group M are penalized in the filament regime rather than in the homogeneous one, since the slope of Q_{micro} versus V associated to these groups is smaller for the blue curve compared to the black ones. This is not the case for Group 3 of the BD, since the increase of Q_{micro} with V is enhanced, especially at the breakdown, meaning that breakdown current microdischarges transport a considerable amount of charges at the highest voltages. Again we can see from Figure 8 that these discharge properties saturate at the highest voltages, since the curves associated to 13.5 kV an 14.6 kV look very similar. Analogous considerations can be done for the forward stroke. In this case Group L is almost absent, Group S is penalized (Figure 9 (a)) and Group M is enhanced (Figure 9 (b)).

For each curve of Figures 8 and 9, the maximum value of Q_{micro} represents the charge totally transported during a backward or forward half-cycle. This quantity is presented in Figure 3 as a function of the voltage amplitude for the different groups of microdischarges. These results suggest that Group S and Group M of the backward stroke together with Group S of the forward stroke determine the increase of the induced wind speed with the voltage amplitude before the transition to the filamentary regime. On the contrary, we can think that microdischarges belonging to Group L of the BD and to Group M of the FD are not effective in generating the wind. In the filamentary plasma regime noticed at the highest voltage amplitudes the importance of the latter groups increases to the detriment of the other groups of microdischarges. The result is that the wind speed saturates even though the total charge transported by the plasma actuator, and thus the consumed power, rises.

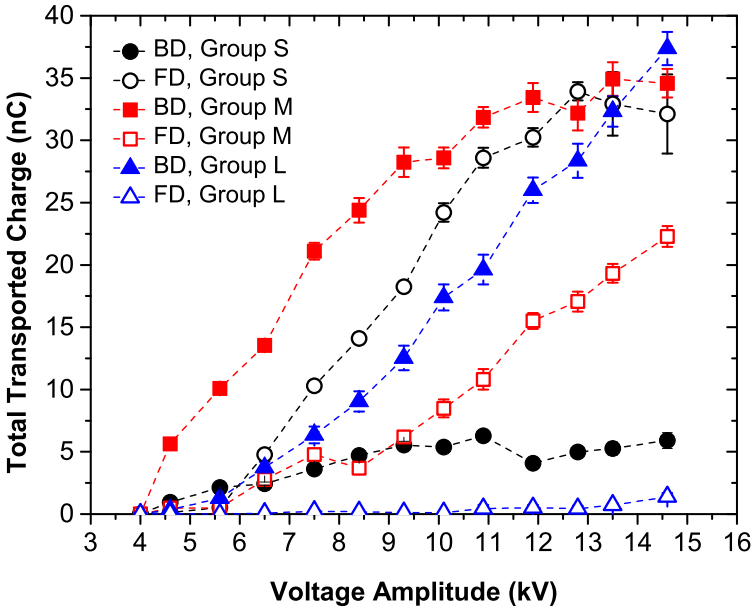

Figure 10. Total charge transported by the different groups of plasma microdischarges during a backward stroke (full symbols) or a forward stroke (blank symbols), as a function of the voltage amplitude. Circles, squares and triangles refer to Group S, Group M and Group L respectively.

4. Conclusions

In this work we have experimentally investigated some properties of an asymmetric surface dielectric barrier discharge fed by a high-voltage sinusoidal low-frequency drive, as a function of the applied voltage. Using a thermal camera and a pitot probe connected to a pressure transducer we have shown that the speed of the flow induced by the SDBD saturates or even decreases when the voltage amplitude is high enough for changing the plasma regime. The new plasma regime can be easily recognised because several plasma filaments are visible and the discharge does not appear uniform any more. We have studied this transition from the point of view of the charge transported by current microdischarges during the backward and forward strokes. We have identified three groups of microdischarges with different temporal duration and results show that they are differently affected by the plasma regime transition. These considerations pave the way for a better understanding of the role played by plasma microdischarges in the creation of the induced airflow. In particular, our analysis suggest that not all these groups of microdischarges effectively contribute to the induced wind generation.

References

[1] Kogelschatz U 2003 *Plasma Chem. Plasma Proc.* **23** 1
[2] Moreau E 2007 *J. Phys. D: Appl. Phys.* **40** 605
[3] Corke T C, Enloe C L and Wilkinson S P 2010 *Annual Rew. Flow Control* **42** 505
[4] Corke T C, Post M L and Orlov D M 2008 *J. Prop and Power* **24** 5
[5] Biganzoli I, Barni R, Riccardi C, Gurioli A and Pertile R 2013 *Plasma Sources Sci. Technol.* **22** 025009
[6] Raizer Y P 1991 *Gas Discharge Physics* (Berlin-Heidelberg: Springer-Verlag)
[7] Biganzoli I, Barni R, Riccardi C, Gurioli A and Pertile R 2013 *J. Phys. D: Appl. Phys.* **46** 2
[8] Orlov D, Font G and Edelstein D 2008 *AIAA J.* **46** 3142
[9] Borghi C A, Cristofolini A, Latini C and Neretti G 2010 *41st Plasmadyn. and Lasers Conf. (Chicago)* 4763
[10] Biganzoli I, Barni R and Riccardi C 2013 *Rev. Sci. Instrum* **84** 016101
[11] Zhang Q, Zhu J, Jia J, Tao F and Yang L 2006 *Meas. Sci. Tech.* **17** 895
[12] Durscher R, Stanfield S and Roy S 2012 *Appl. Phys. Lett.* **101** 252902
[13] Falkestein Z and Coogan J J 1997 *J. Phys. D: Appl. Phys.* **30** 817